Control Trajectory Optimisation and Optimised Control Strategy for an Electric Vehicle HVAC System and Favourable Thermal Comfort

Ivan Cvok*, Branimir Škugor, Joško Deur
University of Zagreb, Zagreb, Croatia
Faculty of Mechanical Engineering and Naval Architecture
e–mail: ivan.cvok@fsb.hr

ABSTRACT

In order to increase the driving range of electric vehicle, while maintaining high thermal comfort inside the passenger cabin, it is necessary to design a control system which optimally synthesizes multiple control actions of heating, ventilation and air-conditioning (HVAC) system, while taking into account various constraints imposed by system hardware requirements. To this end, dynamic programming-based optimisation of HVAC control variables, which simultaneously minimises conflicting criteria of passenger thermal comfort and HVAC efficiency, is first proposed in the paper. Next, a hierarchical structure of thermal comfort control system is proposed, which consists of optimised low-level control loops, a superimposed cabin temperature controller that regulates cooling capacity, and optimisation-based control allocation strategy that sets references for inner HVAC control loop. Finally, the overall control system is verified by simulation for cool-down scenario, and the simulation results are compared with the DP benchmark.

KEYWORDS

Electric vehicle, HVAC, thermal comfort, dynamic-programming, optimisation, optimal control, hierarchical control

INTRODUCTION

In recent years, electric vehicles (EV) have been increasingly adopted by public. Introduction of battery and hybrid electric vehicles enables the automotive engineers to implement a variety of electrically powered components in a single vehicle, which is especially interesting in automotive heating, ventilation and air-conditioning (HVAC) application. Thus, modern electric vehicles are equipped with redundant HVAC actuators and multiple energy flows [1], particularly when considering requirements to implement heat pump systems in addition to A/C system [2]. Furthermore, electric vehicle's driving range is heavily impacted by heating and cooling loads and a significant impact of up to 60% on driving range is reported in cold weather and about 33% in extremely hot weather [3, 4]. The highest contributor to driving range decrease is the vehicles HVAC system, as it can constitute up to 65% of secondary energy consumption, with the primary consumption coming from powertrain. Thus, it is of great interest to achieve a highest possible HVAC system efficiency, which would result in increased driving range, while maintaining high passenger thermal comfort. To fulfil these conflicting criteria, it is necessary to develop advanced control systems which optimally coordinate multiple actuators and energy storage units.

* Corresponding author

Setting a realistic and achievable benchmark for a complex control system is imperative. One of the most common control variable optimisation methods, used for setting control system benchmarks for a specified operating scenario, is dynamic programming (DP). Its main advantage is that it finds globally optimal solution for the general case of a nonlinear, discontinuous and multi-variable system. However, the DP algorithm is rather computationally inefficient, so it can be applied to systems with a low number of state and control variables. DP solutions have been used as benchmark in different types of hybrid electric vehicles, where the aim is to find optimal distribution of control variables (engine and e-motor torques, speeds and clutch state-dependent modes) for minimising fuel consumption while satisfying different hardware constraints including the boundary condition of battery state-of-charge (SoC) at the end of driving cycle [5, 6]. In the framework of HVAC systems, DP has been used in conventional vehicle's A/C system optimisation [7], where an A/C clutch command sequence is optimised to minimise fuel consumption over given driving cycle. The constraints include evaporator outlet air temperature setpoint, and a simple second-order HVAC model.

Cabin thermal comfort is usually indirectly controlled through cabin air temperature control. Fuzzy-logic cabin thermal comfort control based on the simplified predicted mean vote (*PMV*) feedback is presented in [8], where it is shown that both thermal comfort and energy consumption can be improved in comparison with cabin air temperature feedback control. Reference [9] proposes a multi-input, single-output and multi-objective proportional-integral (PI) like controller for cabin thermal comfort control of a conventional vehicle, which accounts for internal combustion engine efficiency and thermal comfort criterion. It is shown therein that the fuel consumption can be reduced compared to conventional control algorithms for the same level of thermal comfort.

In this paper, DP is applied to first-order vehicle cabin model and static HVAC model to obtain the thermal comfort and efficiency benchmark and provide guidelines for cabin thermal comfort control strategy development. The proposed hierarchical control structure consists of superimposed cabin air temperature controller that commands the cooling capacity, optimisation-based control allocation algorithm, and inner HVAC control loops. Control allocation sets references for optimised low-level HVAC controllers and also determines auxiliary control variables such as air mass flow rates by maximising thermal comfort and efficiency, while satisfying HVAC system constraints. Control trajectory optimisation is conducted for a cool-down scenario, and the control strategy performance is verified through simulations for same scenario. Although the presented case study is based on a conventional HVAC system model, the developed optimisation approach and hierarchical control strategy can also be applied to more complex HVAC systems, such as those utilised in advanced fully-electric vehicles (see e.g. [2]).

HVAC AND CABIN MODELLING

The passenger cabin thermal system connected to the conventional HVAC system is depicted in Figure 1. A detailed lumped-parameter control-oriented model of the HVAC system includes 12 state variables related to evaporator ($\mathbf{x}_e$) and condenser ($\mathbf{x}_c$) dynamics [10, 11] which are modelled according to moving-boundary method that provides a good trade-off between model complexity and accuracy. Electric motor-powered compressor, electronic expansion valve, blower fan and condenser fan are considered as typical EV HVAC actuators. They typically have faster dynamics compared to the slower heat exchanger dynamics, which justifies modelling them as static elements [11]. Therefore, control inputs fed to the HVAC model are compressor speed ω_{com}, electronic expansion valve opening a_v, blower fan air mass flow rate $\dot{m}_{ea}$ and condenser fan air mass flow rate $\dot{m}_{ca}$. Outputs of the HVAC model, which are of particular interest in this paper, include evaporator outlet air temperature $T_{ea,out}$ (i.e. cabin inlet air temperature), superheat temperature ΔT_{SH}, and coefficient of performance defined as the ratio of evaporator air-side cooling power and compressor power consumption $COP = \dot{Q}_{ea}/P_{com}$. The power consumption of expansion valve and blower fan is not considered in COP calculation.

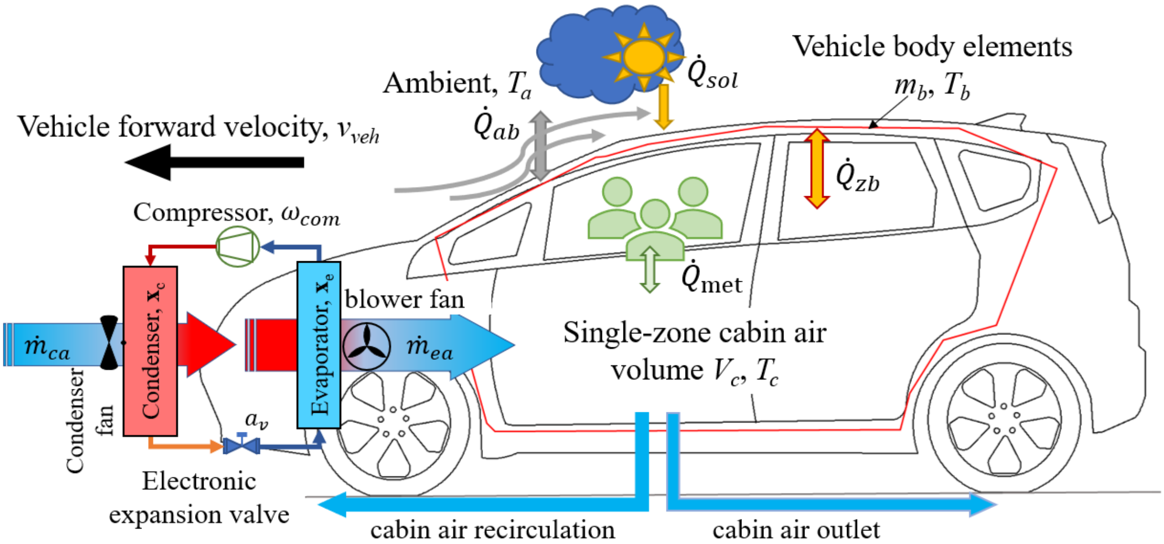

Figure 1. HVAC and cabin model schematic

The considered passenger cabin model [12] consists of two thermal masses: (i) cabin air volume V_c with temperature T_c and (ii) body elements of mass m_b with temperature T_b. The modelled thermal loads include constant metabolic load $\dot{Q}_{met}$ if the cabin air temperature is below 36 °C, solar radiation load $\dot{Q}_{sol}$, ambient air convection heat transfer $\dot{Q}_{ab}$ over outer body surface A_{ab} with variable heat transfer coefficient $\alpha_{ab}(v_{veh})$, HVAC thermal load $\dot{Q}_{HVAC}$ that takes into account cabin air inlet and outlet, and convection heat transfer from body elements to cabin air $\dot{Q}_{cb}$ over inner body surface A_{cb} with heat transfer coefficient α_{cb}. The second-order cabin model obtained by heat balance method [12] then reads:

$$\begin{aligned} c_{pac}\rho_c V_c \dot{T}_c &= \underbrace{\dot{m}_{ea} c_{pae}\left(T_{ea,out}\left(\omega_{com}\right) - T_c\right)}_{\dot{Q}_{HVAC}} + \dot{Q}_{met}\left(T_c\right) + \underbrace{\alpha_{cb} A_{cb}\left(T_b - T_c\right)}_{\dot{Q}_{cb}} \\ c_{pb} m_b \dot{T}_b &= -\underbrace{\alpha_{cb} A_{cb}\left(T_b - T_c\right)}_{\dot{Q}_{cb}} + \dot{Q}_{sol} + \underbrace{\alpha_{ab}\left(v_{veh}\right) A_{ab}\left(T_b - T_a\right)}_{\dot{Q}_{ab}} \end{aligned} \tag{1}$$

where c_{pa} is the air specific heat capacity, ρ_c is the air density and c_{pb} is the body specific heat capacity.

The second-order cabin model (1) can further be simplified to first order model by assuming that the body temperature dynamic is slower than the cabin air temperature dynamic, which gives:

$$\begin{aligned} &k_c c_{pa} \rho_c V_c \dot{T}_c = \underbrace{\dot{m}_{ea} c_{pae}\left(T_{ea,out}\left(\omega_{com}\right) - T_c\right)}_{\dot{Q}_{HVAC}} + \dot{Q}_{met}\left(T_c\right) + \dot{Q}_{sol} + \underbrace{\alpha_{ab}\left(v_x\right) A_{ab}\left(T_a - T_b\right)}_{\dot{Q}_{ab}} \\ &T_b = T_c + \Delta T_b \le T_{b,\max} \end{aligned} \tag{2}$$

where k_c scales the cabin air temperature thermal inertia to match the second order model dynamics and ΔT_b is the air-to-body temperature offset used for “tuning” the steady state accuracy.

Since cabin models consider complete cabin volume, it is assumed that the mean air velocity v_{air} inside the cabin is proportional to the blower fan air mass flow rate $\dot{m}_{ea}$:

$$v_{air} = k_{mve}\dot{m}_{ea} \tag{3}$$

where k_{mve} is proportionality constant e.g. expressed as the ratio of air density and cabin inlet vents cross-section area. Similarly, a linear relationship between the vehicle speed v_{veh} and the condenser fan air mass flow rate $\dot{m}_{ca}$ is assumed:

$$\dot{m}_{ca} = \dot{m}_{ca0} + k_{mvc}v_{veh} \tag{4}$$

where $\dot{m}_{ca0}$ is air mass flow rate for stationary vehicle and k_{mvc} is constant coefficient. The closed-loop dynamics of evaporator outlet air temperature control system of the particular HVAC model is by an order of magnitude faster than the cabin air temperature dynamics. In order to enhance computational efficiency of DP-based control variable optimisation, the HVAC is represented by static maps which describe steady-state input to output relationships. The static maps shown in Figure 2 have been obtained by a numerical method/tool described in [11] for the superheat temperature being fixed to its target value of 5 °C (it is assumed that the superheat temperature is effectively controlled by the expansion valve) and the 12th-order model presented therein.

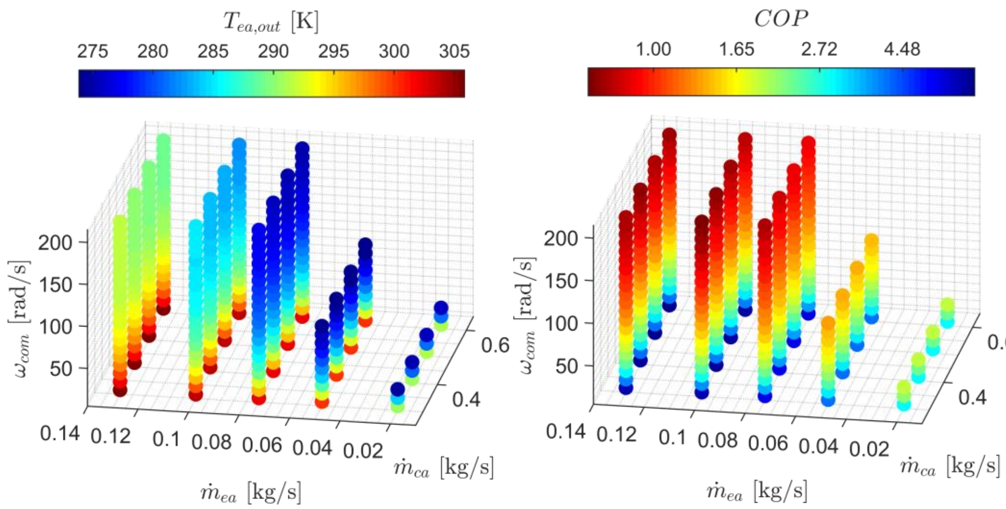

Figure 2. HVAC model static maps related to evaporator outlet air temperature (a) and efficiency defined by COP (b)

The cabin thermal comfort is evaluated through Predicted Mean Vote (PMV), which is adjusted to take into account the cooling effect of increased air velocity [13]. A positive PMV means that the cabin environment is too hot, while a negative PMV indicates that it is too cold. The zero PMV suggests ideal thermal comfort, while the comfortable range is defined as $|PMV| < 0.5$ [13]. PMV takes into account six different parameters: air temperature T_{air}, air velocity v_{air}, mean radiant temperature, air relative humidity RH, clothing, and metabolic rate. In order to simplify the PMV calculation, it is assumed that the driver is wearing summer clothes and that the mean radiant temperature is equal to the mean air temperature inside the cabin. The PMV map shown in Figure 3a is obtained for the relative humidity $RH \in [0, 1]$, air temperature $T_{air} \in [16, 40]$ °C, air velocity $v_{air} \in [0.17, 1.1]$ m/s, clothing thermal resistance of 0.5 clo, and metabolic rate of 1.5 (typical value for driving) [13]. Black circles indicate comfort range, i.e. $|PMV| < 0.5$. An example of PMV map for the constant relative humidity of 44% is shown in Figure 3b, where the black solid lines denote the boundaries of comfort range ($|PMV| < 0.5$), shows that the same thermal comfort can be achieved with higher cabin air temperature if the air velocity is increased (and also if the humidity is reduced, Fig. 3a)

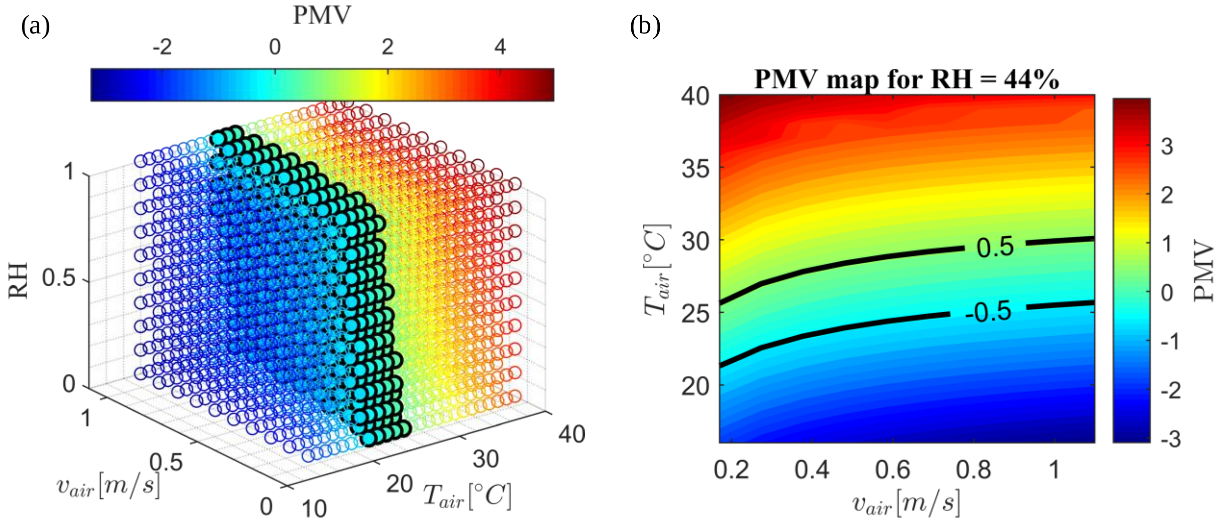

Figure 3. Predicted mean vote (*PMV*) map with three inputs where filled circles show comfort range (|*PMV*| < 0.5) (a) and *PMV* map with two inputs and fixed relative humidity (*RH* = 44%) where black lines denoting comfort range (b)

CONTROL VARIABLE OPTIMISATION

The presented control variable optimisation approach is based on the dynamic programming (DP) optimisation algorithm [14]. DP optimisation results in globally optimal solution as it starts with final time t_f and calculates optimal control inputs for all possible state variables (satisfying the process model) backwards in time at each time instant. However, DP is computationally very expensive and the computational cost exponentially grows with the number of state variables and control inputs. Therefore, discrete-time counterpart of the first order cabin air temperature model defined by Equation (2) is used in DP optimisation to describe single state-variable (x) dynamics:

$$x = T_c,$$

with two control inputs contained in control vector **u**:

$$\mathbf{u} = \begin{bmatrix} \omega_{com} & \dot{m}_{ea} \end{bmatrix},$$

while the condenser fan air mass flow rate $\dot{m}_{ca}$ represents disturbance variable (potentially, it could be included in optimisation as an additional control variable). The HVAC evaporator outlet air temperature $T_{ea,out} = T_{ea,out}(\omega_{com}, \dot{m}_{ea}, \dot{m}_{ca})$ and efficiency $COP = COP(\omega_{com}, \dot{m}_{ea}, \dot{m}_{ca})$ are described by the static maps depicted in Figure 2, where a trilinear interpolation is applied for input combinations that are not defined by the map). The expansion valve opening a_v is not contained in control vector **u** since the HVAC static maps have been obtained for constant/target superheat temperature value. The thermal comfort criterion *PMV* is obtained by map shown in Figure 3a, where the trilinear interpolation is again applied for the case of missing input combinations.

The control variable optimisation problem is to find the control vector **u**(k), which minimises the cost function J:

$$J = \Phi\left(x\left(t_f\right)\right) + \sum_{k=1}^{N} F\left(x\left(k\right), \mathbf{u}\left(k\right)\right) \tag{5}$$

at each discrete-time instant k, where the terminal condition function:

$$\Phi\left(x\left(t_f\right)\right) = K_{penf}\left(x_{tf,R} - x\left(t_f\right)\right)^2 \tag{6}$$

ensures that the cabin air temperature reference $x_{tf,R} = T_{c,R}$ is achieved at the end of optimisation time horizon, by applying sufficiently high penalisation coefficient K_{penf}. The sub-integral function $F(\cdot)$ includes minimisation of thermal comfort criterion (*PMV*) and maximisation of efficiency (*COP*), alongside with penalisation of state-variable and control inputs constraint violations:

$$\begin{aligned} &F\left(x(k),\mathbf{u}(k)\right) = K_{PMV}\left|PMV(\mathrm{k})\right| + K_{COP}COP(k)^{-1} + \\ &K_{pen}\left[H\left(x(k)-x_{\max}\right)+H\left(x_{\min}-x(k)\right)\right]+K_{pen}\left[H\left(\mathbf{u}(k)-\mathbf{u}_{\max}\right)+H\left(\mathbf{u}_{\min}-\mathbf{u}(k)\right)\right] \end{aligned} \tag{7}$$

where K_{PMV} and K_{COP} are weigthing coefficients that set the trade-off between thermal comfort and efficiency, K_{pen} is constraint violation penalisation coefficient that should be sufficiently high, and $H(a)$ is Heaviside function defined as $H(a) = 0$ for $a < 0$ and $H(a) = 1$ for $a \geq 1$. Constraints are used to contain the state-variable in the target range and use control inputs that are within specified hardware-related limits.

CONTROL STRATEGY DESIGN

The control strategy proposed in this paper has a two-level hierarchical (cascade) structure (see Fig. 6). Low-level feedback controllers ensure setpoint tracking and disturbance rejection for HVAC subsystem. The high-level control subsystem controls the cabin air temperature and allocates references for low-level controllers.

Low-level control system

The evaporator outlet air temperature (i.e. the cabin inlet air temperature) $T_{ea,out}$ is controlled in a feedback loop to provide accurate and high-bandwidth tracking of the reference set by the high-level control system. The superheat temperature ΔT_{SH} is regulated with respect to fixed reference $\Delta T_{SH,R}$ = 5 °C (a safety function), where the main aim of the corresponding feedback controller is to suppress disturbance influence including the one imposed by the action of outlet temperature controller. The linearized input-output HVAC model depicted in Figure 4a is characterised by coupled dynamics, which can be described by four transfer functions linking the control inputs (compressor speed ω_{com} and expansion valve opening a_v) and controlled outputs (evaporator outlet air temperature $T_{ea,out}$ and superheat temperature ΔT_{SH}):

$$G_{11}(s)=\frac{T_{ea,out}(s)}{\omega_{com}(s)},\quad G_{12}(s)=\frac{T_{ea,out}(s)}{a_v(s)},\quad G_{21}(s)=\frac{\Delta T_{SH}(s)}{\omega_{com}(s)},\quad G_{12}(s)=\frac{\Delta T_{SH}(s)}{a_v(s)}. \tag{8}$$

Reasonably good control performance of superheat temperature regulation and evaporator setpoint tracking can be obtained for the given HVAC model by applying a simplified, decoupled control structure where only two main controllers $G_{c11}(s)$ and $G_{c22}(s)$ are used (Fig. 4a; there are no cross-coupling control actions). The controllers are of proportional-integral (PI) type, and their parameters are tuned by using a search-algorithm optimisation procedure targeted to single-input single-output (SISO) system [15]. The cost function to be minimised combines penalisation of closed-loop control error and control effort Referring to control structure shown in Fig. 4a, the cost functions for the two control loops are defined as:

$$\begin{aligned} \min J_{11} &= \frac{1}{1+M}\sum_{k=0}^{M}\left[\left(T_{ea,out,R}-T_{ea,out}\right)^2 + r_{11}\left(\omega_{com,R}-\omega_{com}\right)^2\right] \\ \min J_{22} &= \frac{1}{1+M}\sum_{k=0}^{M}\left[\left(\Delta T_{SH,R}-T_{SH}\right)^2 + r_{22}\left(a_{v,R}-a_v\right)^2\right] \end{aligned} \tag{9}$$

where r_{11} and r_{22} are weighting coefficients which set the trade-off between control error suppression (performance) and control effort reduction (efficiency, relative stability). Since the HVAC dynamics model parameters depend on the operating point, gain scheduling maps (two proportional gain maps K_{p11} and K_{p22}, and two integral gain maps K_{i11} and K_{i22}) have been obtained by repeating the PI controller parameter optimisation procedure for multiple operating points with fixed weighting coefficients r_{11} and r_{22}. The analysis showed that the most significant operating point parameters were the evaporator outlet air temperature $T_{ea,out}$ and the blower fan air mass flow rate $\dot{m}_{ea}$, which results in two-dimensional gain scheduling maps $K_x = f_x(T_{ea,out}, \dot{m}_{ea})$. Final low-level control system structure is shown in Figure 4b and consists of two PI controllers with two pairs of gain-scheduling maps.

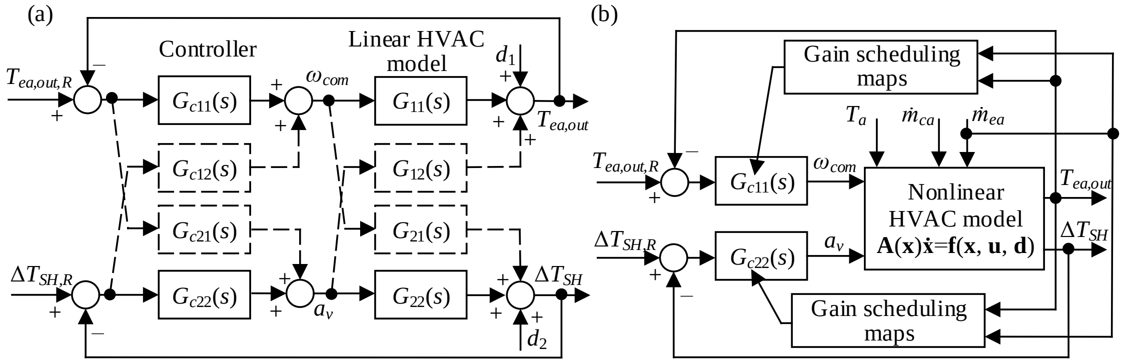

Figure 4. Block diagram of linearized HVAC system and controllers (solid lines) used in controller parameter optimisation (where d denotes disturbance, e.g. varying air mass flow rate) (a), and block diagram of final low-level control system (b)

The low-level control system performance is illustrated in Figure 5 for the full, 12-th order nonlinear process model, where blue lines denote the performance of control system with fixed controller gains (tuned for $T_{ea,out}$ = 15 °C and m_{ea} = 0.05 kg/s), while green lines correspond to the control system with gain-scheduling applied. The evaporator air mass flow rate m_{ea} is kept at 0.075 kg/s, the superheat temperature reference is set to $\Delta T_{SH,R}$ = 5 °C and the step reference with magnitude of $\Delta T_{ea,out,R}$ = 5 °C is applied at t = 1000 s. In comparison with the control system that uses fixed controller gains, the control system with gain scheduling achieves faster evaporator outlet air temperature response (Fig. 5a), and lower superheat temperature control error (Fig. 5b). The performance improvement is achieved by stronger compressor and expansion valve control efforts (Figs. 5c and 5d). Figures 5e and 5f show that optimal controller gains vary significantly throughout the operating range, thus making the gain scheduling algorithm necessary to achieve optimal performance over a wide operating range.

It has been found that the closed-loop system performance can be further improved by taking into account the coupled dynamics of HVAC model, which is determined in Figure 4a by the cross-coupling transfer functions $G_{12}(s)$ and $G_{21}(s)$. In this case, the parameters of both PI controller were optimized simultaneously, with an option to include the cross-coupling gains as well (see $G_{c12}(s)$ and $G_{c21}(s)$ in Fig. 4a). A multi-objective genetic algorithm was used as optimisation algorithm, because it allows for overcoming the issue of local optima appearance and can present the results in the form of Pareto frontier that enable the designer to select optimal solution based on his/her preference. However, such procedure is more time consuming, especially when gain-scheduling is concerned, and it is not presented here due to paper length constraints.

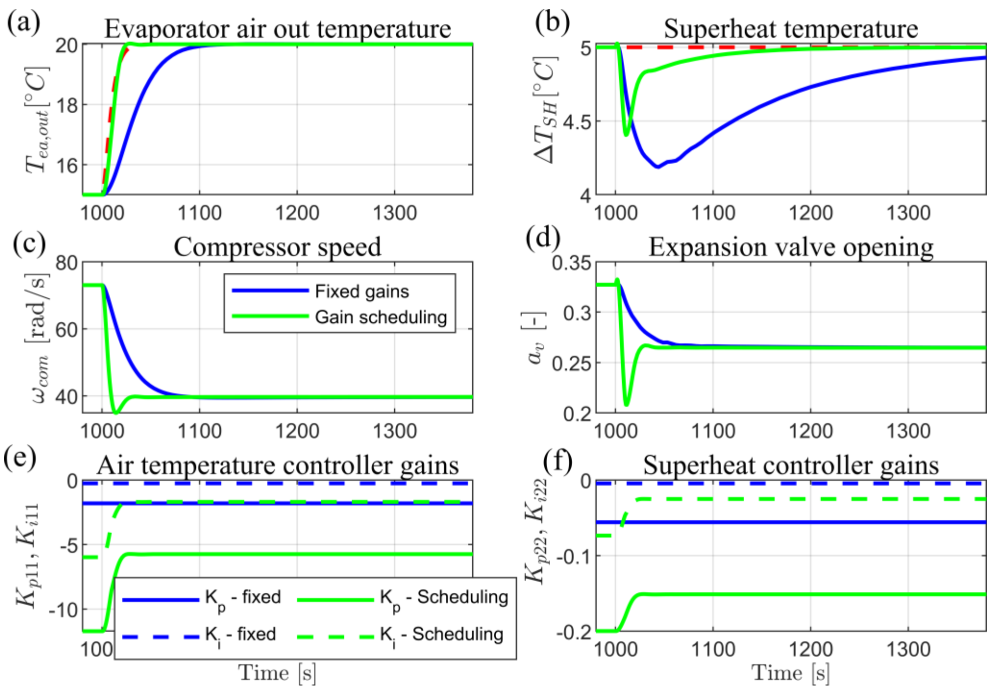

Figure 5. Comparison of low-level controller performance with and without using gain scheduling maps.

High-level control system

In order to achieve favourable thermal comfort inside the vehicle cabin while maintaining best possible efficiency of the HVAC system, a supervisory high-level control system has been developed. According to the block diagram shown in Figure 6, the high-level control system regulates the cabin air temperature T_c by commanding the cooling capacity $\dot{Q}_d$. The cooling capacity $\dot{Q}_d$ is then transformed to low-level controller inputs/references, which in this case include evaporator outlet air temperature reference $T_{ea,out,R}$ and air mass flow rate $\dot{m}_{ea,R}$ (while in a more general case more inputs are possible, such as $\dot{m}_{ca,R}$ in Fig. 6). It is crucial that, in order to achieve optimal system performance, the design of control allocation map should be based on use of optimisation. Discrete-time PI-type cabin air temperature controller $G_{c,CAB}(z)$ with fixed gains is used in this paper (with an option to add the gain scheduling algorithm in more general case). Since the cabin air temperature dynamics are slow, the cabin air temperature controller and control allocation strategy can have higher sampling time than the low-level controllers (e.g. 10 s vs. 0.1 s).

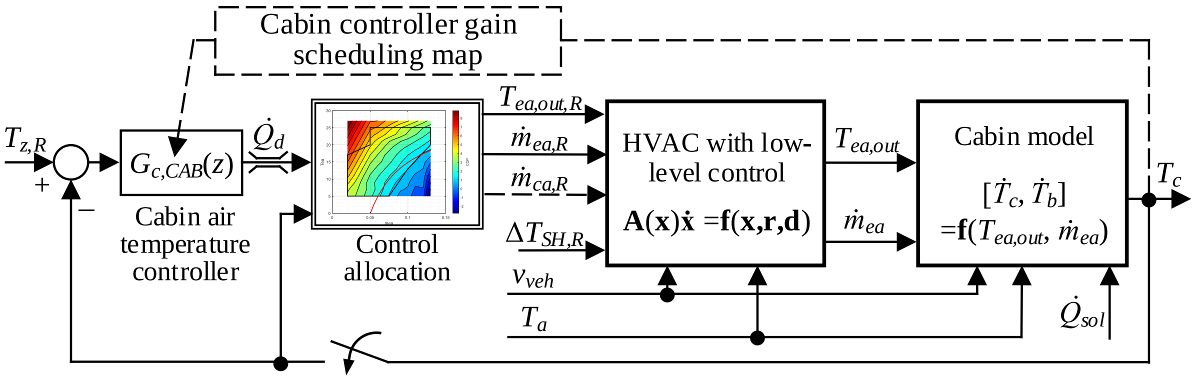

Figure 6. Cabin air temperature control block diagram

The optimal control allocation map is obtained by minimising the following cost function for a wide range of operating points ($\dot{Q}_d$, T_c):

$$J_{ca} = K_{PMV} \left| PMV\left(\dot{m}_{ea,R}, T_c\right) \right| + K_{COP} \frac{1}{COP\left(\dot{m}_{ea,R}, T_{ea,out,R}\right)} \tag{10}$$

where K_{PMV} and K_{COP} are weighting coefficients that set the trade-off between the two conflicting criteria: thermal comfort (*PMV*) and efficiency (*COP*). Control variables are subject to following constraints:

$$\begin{gathered} \dot{Q}_d = \dot{m}_{ea,R} c_{pa} \left(T_{ea,out,R} - T_c\right) \\ \dot{m}_{ea,R,\min} \le \dot{m}_{ea,R} \le \dot{m}_{ea,R,\max} \\ T_{ea,out,R,\min}\left(\dot{m}_{ea,R}\right) \le T_{ea,out,R} \le T_{ea,out,R,\max}\left(\dot{m}_{ea,R}\right) \end{gathered} \tag{11}$$

where c_{pa} is the specific heat capacity of air, $\dot{Q}_{d,\max}$ is maximum cooling capacity that can be achieved by HVAC system at the specified cabin air temperature, $\dot{m}_{ea,R,\max}$ and $\dot{m}_{ea,R,\min}$ are maximum and minimum air mass flow rates, and $T_{ea,out,R,\max}$ and $T_{ea,out,R,\min}$ are maximum and minimum evaporator outlet air temperatures that can be attained at certain air mass flow rate.

RESULTS

Control variable optimisation (and, similarly, control system simulation analysis) have been carried out for cool-down scenario at constant vehicle velocity v_{veh} = 40 km/h. The objective of the cool-down scenario is to bring the cabin air temperature down from its initial value that is equal to ambient air temperature $T_{c0} = T_a$ = 40 °C to the final cabin air temperature of $T_{c,R}$ = 26 °C in 10 minutes, i.e. t_f = 600 s.

Control variable optimisation results

Dynamic programming has been carried out with the time step Δt = 1 s (number of time samples N_t = 601). The state variable (cabin air temperature) has been discretized with the resolution of 0.5 °C in the range from 20 °C to 40 °C, the evaporator air mass flow rate discretization step is 0.01 kg/s between 0.02 kg/s and 0.13 kg/s, and the compressor speed discretization step is 5 rad/s between 10 rad/s and 210 rad/s.

Three different optimisation cases that have been considered are: (i) *PMV* minimisation (K_{PMV} = 1 and K_{COP} = 0 are set in the cost function (7)), (ii) *COP* maximisation (K_{PMV} = 0 and K_{COP} = 1), and (iii) combined case of simultaneous *PMV* minimisation and *COP* maximisation (K_{PMV} = 0.5 and K_{COP} = 1). The results shown in Figure 7 indicate that for the case of *COP* maximisation (red line), the optimal control is such to keep the compressor speed low (Fig. 7d) and to slowly increase it through time to eventually bring the cabin temperature towards its reference value (dashed line in Fig. 7a). Due to the low compressor speed and a modest cooling power (a relatively slow fall of cabin air temperature), the evaporator air mass flow rate (Fig. 7c) should be relatively high. For the case of *PMV* minimisation, the optimal control behaviour is to increase the compressor speed and air mass flow rate (Figs. 7d and 7c) at the beginning of response, in order to lower the cabin inlet air temperature (Fig. 7a) and bring the thermal comfort criterion *PMV* (Fig. 7e) towards zero as fast as possible. This results in the lowest *COP* (Fig. 7f) until the thermal comfort has been achieved (*PMV* =0), and afterwards the *COP* increases as lower compressor speed and lower air mass flow rate are sufficient to maintain the *PMV* around zero. In the combined cost function case (green line), optimal control expectedly results in compromise between the previous two extreme cases.

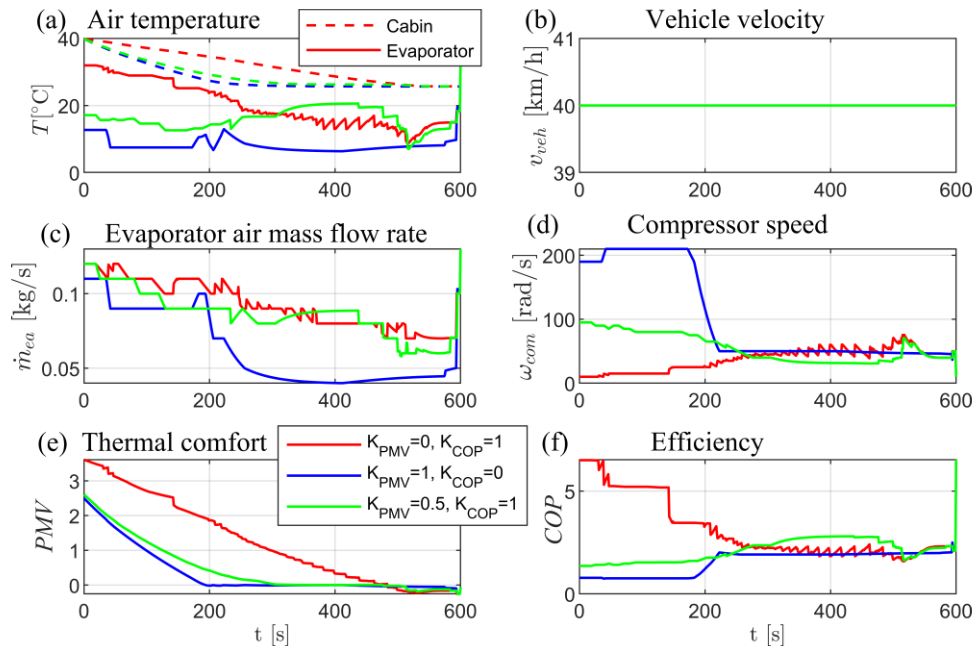

Figure 7. Control variable optimisation results for three optimisation cases: *PMV* minimisation only (blue), *COP* maximisation only (red) and combined PMV minimisation and COP maximisation (green)

Control strategy results

Control strategy simulation results shown in Figure 8 have been obtained for three characteristic cases of tuning the cost function (10) used in control allocation optimisation: *PMV* minimisation (K_{PMV} = 1 and K_{COP} = 0), (ii) *COP* maximisation (K_{PMV} = 0 and K_{COP} = 1), and (iii) combined case of simultaneous *PMV* minimisation and *COP* maximisation (K_{PMV} = 0.5 and K_{COP} = 1) with fixed cabin temperature PI controller gains K_p = 125, K_i = 0.01. Cabin air temperature response shown in Figure 8a (dashed lines) is similar for all three cases due to the same PI controller used. However, the allocated control inputs, i.e. the evaporator outlet air temperature shown (Fig. 8a, solid lines) and the evaporator air mass flow rate (Fig. 8f), are dependent on weighting coefficients K_{PMV} and K_{COP}. For the case of *COP* maximisation (red line), the compressor speed (Fig. 8c) is kept low, which results in highest efficiency (Fig. 8e, dashed lines), similarly to DP results shown in Figure 7. However, the evaporator air mass flow rate (Fig. 8f) is kept low here, in order to lower the cabin air inlet temperature (Fig. 8a, solid lines) i.e. to meet the high cooling capacity demand, which was not the case in Fig. 7. For the case of *PMV* minimisation (blue line) thermal comfort (Fig. 8e, solid lines) is achieved at fastest rate but this case results in lowest efficiency. The results of combined cost function case (green line) fall between previous two extreme cases, which was also the case in control variable optimisation. Figures 8b and 8d show that the performance of superheat temperature control is satisfying, and it could be further improved by applying more complex cross-coupling control.

The performance of high-level control strategy in terms of transient behaviour of cabin air temperature highly depends on cabin air temperature PI controller parameters. Figure 9 shows simulation results for three different PI controller integral gain tunings: K_i = 0.005 (red line), K_i = 0.01 (green line) and K_i = 0.02 (blue line) and the combined-criteria cost function (K_{PMV} = 0.5, K_{COP} = 1). The cabin air temperature response (Fig. 9a, dashed lines) is faster for higher integral gain K_i, because the cooling capacity demand effort is higher (Fig 9b). This also results in faster thermal comfort achievement but deteriorates efficiency (cf. Fig. 9c). The increased cooling capacity demand (higher K_i) is optimally satisfied with lower evaporator outlet air mass flow rate (Fig. 9e) which enables lower evaporator air outlet temperature (Fig. 9a, solid lines). Fig. 9d shows distribution of operating points over the *COP* map, from which follows that slowest PI controller tuning results in highest efficiency as the operating points in that case are grouped further to the left (higher *COP*).

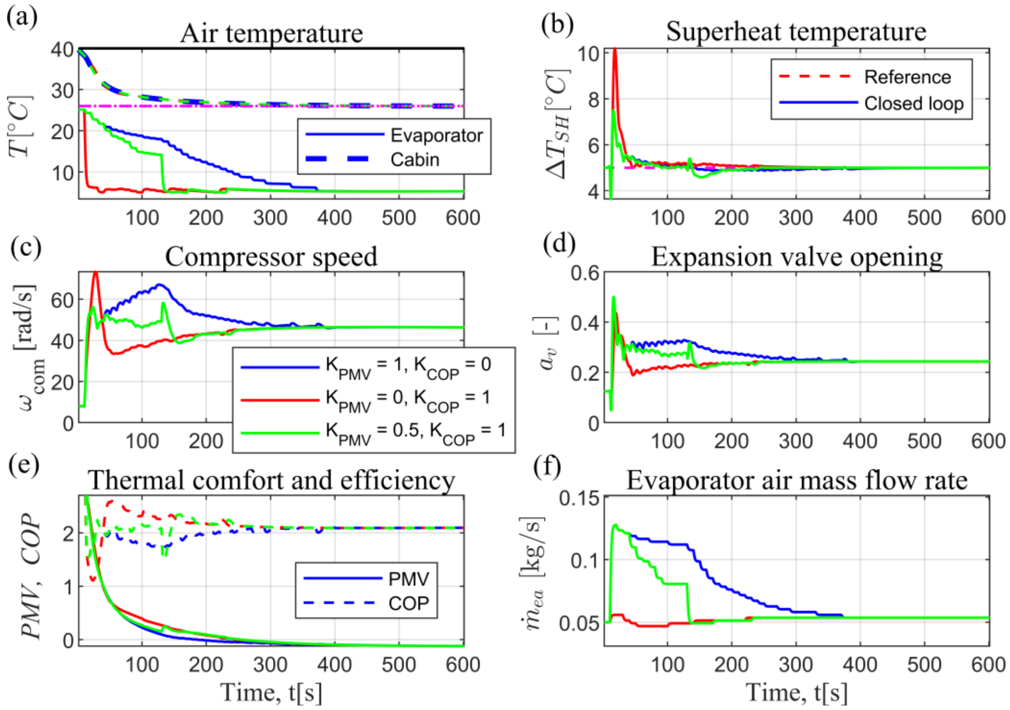

Figure 8. Control strategy simulation results for the case of *PMV* minimisation (blue line), *COP* maximisation (red line) and combined cost function case (green line); the superimposed cabin temperature controller has the fixed parameters.

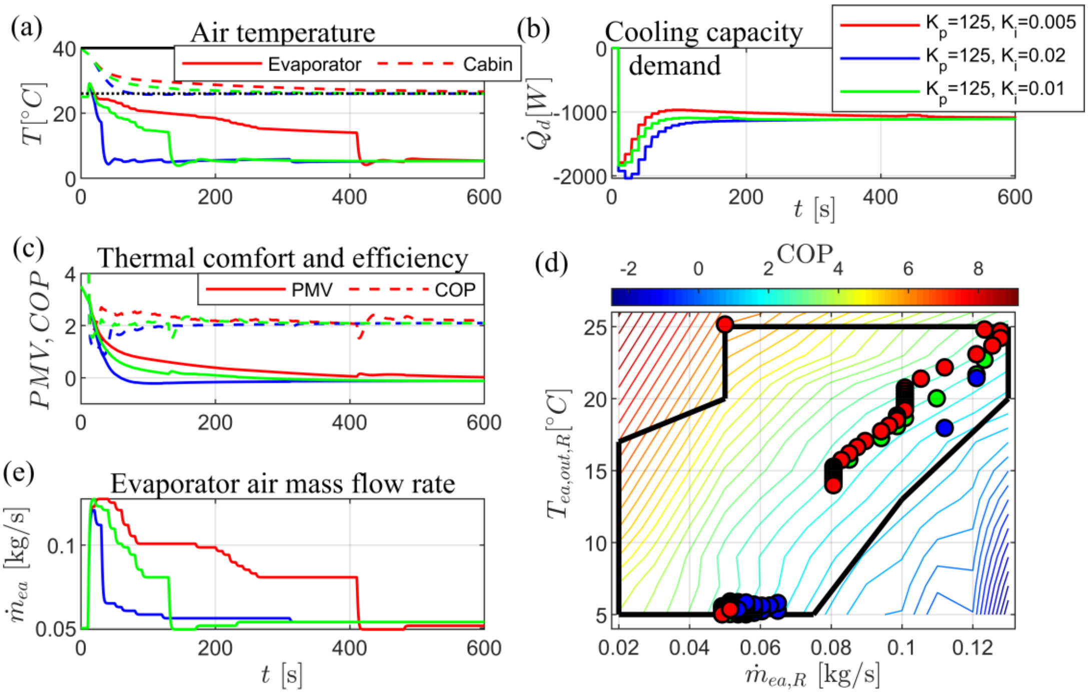

Figure 9. Control strategy simulation results for the case of three different PI controller tunings: K_i = 0.005 (red line), K_i = 0.01 (green line) and K_i = 0.02 (blue line), while the PMV vs. COP trade-off is fixed (to combined penalization).

The above analysis of the results presented in Fig. 9 imply that besides the penalization factors K_{PMV} and K_{COP} of cost function (10), the cabin air temperature controller tuning can be effectively used in setting the trade-off between thermal comfort and efficiency to bring the controller performance even closer to the DP benchmark. Additionally, it suggests that different hierarchical structures might be worth considering, e.g. focusing the allocation on *COP* maximisation and setting the thermal comfort by varying the bandwidth of air temperature controller, or possibly including a *PMV* controller instead of cabin air temperature controller.

CONCLUSION

A hierarchical thermal comfort control strategy including optimisation-based control allocation algorithm that accounts for vehicle HVAC system efficiency has been developed and compared with globally optimal dynamic programming-based control variable optimisation results. Analysis of the results shows that it is possible to achieve favourable trade-off between thermal comfort and HVAC efficiency in optimisation-based feedback control strategy that is qualitatively comparable to globally optimal solution by properly tuning the control strategy parameters (in this case, the optimal allocation cost function weighting coefficients and superimposed cabin temperature controller bandwidth/gains).

Ongoing work includes extending the control variable optimisation tool with (i) additional state-variables to take into account possibly slower HVAC dynamics that could occur with different HVAC system architectures, and (ii) including additional control variables that may improve the system performance. Similarly, optimisation-based control allocation strategy performance improvements related to inclusion of additional control inputs and corresponding tuning of cabin air temperature controller parameters are an ongoing activity. Finally, a thorough multi-objective optimisation-based low-level controller tuning/scheduling, taking into account coupled HVAC dynamics, should be considered as a final refinement of the overall control strategy.

ACKNOWLEDGEMENT

It is gratefully acknowledged that this work has been supported through QUIET project (Qualifying and implementing a user-centric designed and efficient electric vehicle), which has received funding from the European Union’s Horizon 2020 Research and Innovation Programme under Grant agreement No. 769826. In addition, the research work of the first author has been partly supported by the Croatian Science Foundation through the "Young researchers’ career development project – training of new doctoral students".

REFERENCES

1. Zhang, Z., Wang, J., Feng, X., Chang, L., Chen, Y., Wang, X., The Solutions to Electric Vehicle Air Conditioning Systems: A Review, Renew. Sustain. Energy Rev., 91, pp 443-463, 2018
2. Drage, P., Hinteregger, M., Zotter, G., Šimek, M., Cabin Conditioning for Electric Vehicles, ATZ Worldwide, Vol. 121, No. 2, pp 44-49, 2019
3. Zhang, T., Gao, C., Gao, Q., Wang, G., Liu, M.H., Guo, Y., Xiao, C., Yan, Y.Y., Status and Development of Electric Vehicle Integrated Thermal Management from BTM to HVAC, Appl. Therm. Eng., Vol. 88, pp. 398-409, 2015
4. Paffumi, E., Otura, M., Centurelli, M., Casellas, R., Brenner, A., Steffen, J., Energy Consumption, Driving Range and Cabin Temperature Performances at Different Ambient Conditions in Support to the Design of a User-Centric Efficient Electric Vehicle: the QUIET Project, 14th SDEWES Conference, Dubrovnik, 2019

5. Guzella, L., Sciaretta, A., *Vehicle Propulsion Systems*, Springer, Berlin, 2007
6. Škugor, B., Cipek, M., Deur, J., Control Variables Optimization and Feedback Control Strategy Design for the Blended Operating Regime of an Extended Range Electric Vehicle, SAE Int. J. Altern. Powertrains. Vol. 3, pp. 152-162, 2014
7. Zhang, Q., Stockar, S., Canova, M., Energy-Optimal Control of an Automotive Air Conditioning System for Ancillary Load Reduction, IEEE Trans. Control Syst. Technol., Vol. pp 67-80, 2016.
8. Farzaneh, Y., Tootoonchi, A.A., Controlling Automobile Thermal Comfort using Optimized Fuzzy Controller, Appl. Therm. Eng., Vol. 28, No. 14, pp. 1906-1917, 2008
9. Yan, X., Felming, J., Lot, R., A/C Energy Management and Vehicle Cabin Thermal Comfort Control, IEEE Trans. Veh. Technol., Vol. 67, No. 11, pp. 11238-11242, 2018
10. Jensen, J.M., Tummerscheit, H., Moving Boundary Models for Dynamics Simulations of Two-Phase Flows, in: 2nd Int. Model. Conf., pp. 235-244, 2002
11. Ratković, I., Cvok, I., Soldo, V., Deur, J., Control-oriented Modelling of Vapour Compression Cycle Including Model-order Reduction and Analysis Tools, 14th SDEWES Conference, Dubrovnik, 2019
12. Fayazbakhsh, M.A., Bahrami, M., Comprehensive Modeling of Vehicle Air Conditioning Loads Using Heat Balance Method, in: SAE Tech. Pap. 2013-01-1507, 2013.
13. ASHRAE Standard, "Thermal Environmental Conditions for Human Occupancy", ANSI/ASHRAE Standard 55, Rev. 2017
14. Bellman, R. E., Dreyfus, S. E., *Applied Dynamic Programming*, Princeton University Press, New Jersey, 1962
15. Isermann, R., *Digital Control Systems*, Springer-Verlag Berlin Heidelberg, Berlin, 1981